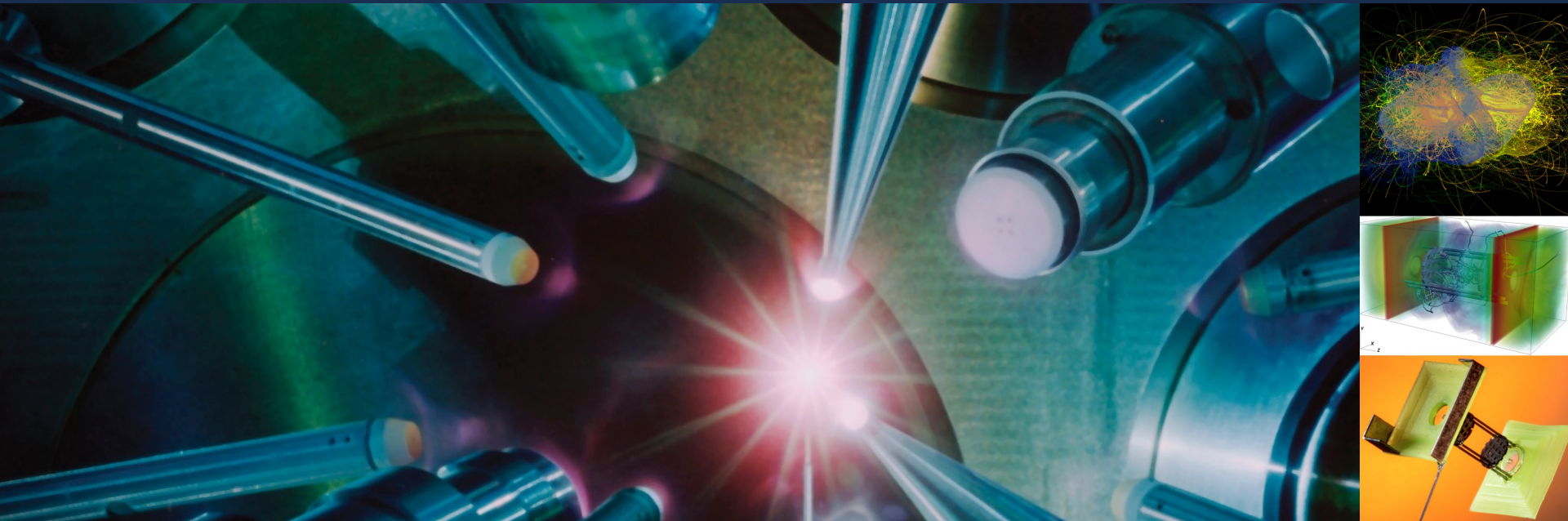


Strong Suppression of Heat Conduction in Laser-driven Magnetized Turbulent Plasmas



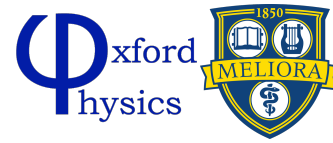
Petros Tzeferacos

Flash Center for Computational Science
Department of Physics and Astronomy
Laboratory for Laser Energetics
University of Rochester

63rd Annual Meeting of the
APS Division of Plasma Physics
November 8–12, 2021
Pittsburgh, PA
Abstract: UO03.00010



TDYNO Collaboration



P Tzeferacos, A Reyes, Y Lu, A Armstrong, K Moczulski



G Gregori, J Meinecke, H Poole, L Chen, T Campbell, A Bell, S Sarkar, F Miniati, A Schekochihin



D Lamb



D Froula, J Katz, D Haberberger, D Turnbull, S Fess (and all LLE staff really!)



H-S Park, JS Ross, T Doepfner, J Emig, C Goyon, D Ryutov, B Remington, A Zylstra



C-K Li, A Birkel, R Petrasso, H Sio, F Seguin

A Bott (Princeton), C Palmer (QUB), B Khair (ONERA), S Feister (CSUCI), A Casner (CEA), D Ryu (Unist), B Reville (MP), C Forest (U Wisconsin), J Foster (AWE), Y Sakawa (Osaka), F Fiuza (SLAC), E Churazov (MPIA), R Bingham (RAL), T White (U Nevada Reno), E Zweibel (U Wisconsin)

Thanks to our sponsors



Engineering and Physical Sciences Research Council

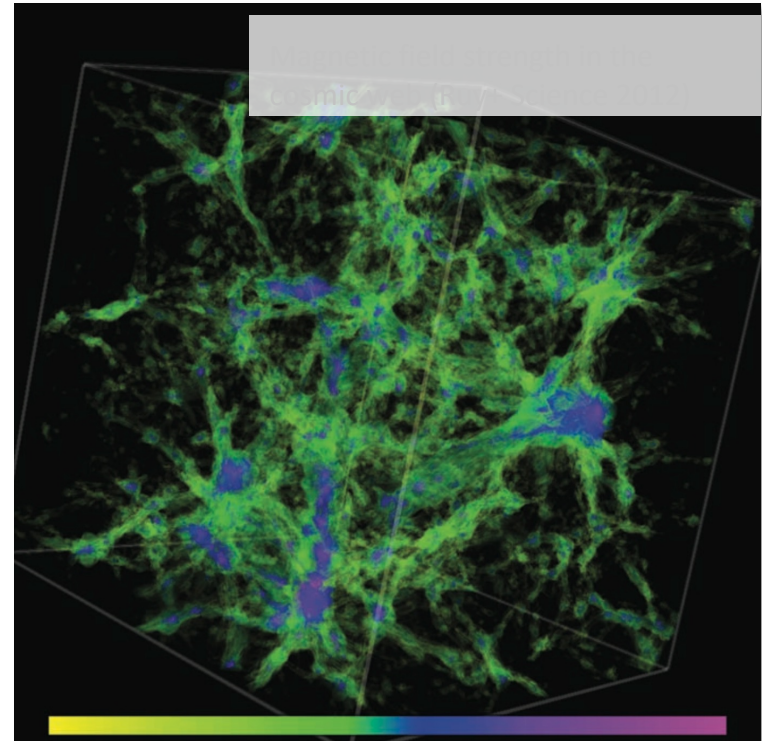
- DOE NNSA, DOE Office of Science, NSF, EPSRC
- DOE's INCITE & ALCC (@ANL), NLUF (@LLE) & DS (@LLNL)
- DOE NNSA NLUF: **DE-NA0002724, DE-NA0003605, DE-NA0003934**
- NSF/DOE Partnership in Basic Plasma & Engineering: **PHY-2033925**
- and General Atomics for target R&D and manufacturing!



Lawrence Livermore National Laboratory

- ❑ The advent of high-power lasers has opened **new fields of plasma physics research** and has enabled the reproduction of **astrophysical environments in the laboratory**.
- ❑ The TDYNO platform, which was designed with FLASH simulations to **demonstrate fluctuation dynamo in the lab for the first time**, at the Omega Laser Facility at the Laboratory for Laser Energetics (Tzeferacos+ 2018), has been successfully ported onto the **National Ignition Facility** (Meinecke et al. submitted, arXiv:2105.08461).
- ❑ The NIF experiments achieve fluctuation dynamo in the **large magnetic Prandtl number regime**, an experimental replica for the magnetized turbulence in the IGM.
- ❑ The **strong magnetic fields** generated in the experiments resulted in a **reduction of local heat transport by two orders of magnitude or more**, leading to strong temperature variations on small spatial scales, as is seen in cluster plasmas (Markevitch+ 2003).

- ❑ Galaxy clusters are diffuse, turbulent magnetized plasmas.
- ❑ In cluster cores, **the temperatures remain anomalously high** compared to what might be expected, given that **the cooling time is short** relative to the Hubble time.
- ❑ While feedback from the central active galactic nuclei is believed to provide most of the heating, there has been **a long debate** as to whether conduction of heat from the bulk to the core might help the core reach observed temperatures.
- ❑ Thermal conduction in magnetized, weakly collisional plasmas is **a longstanding problem in ICF and fusion research.**





UNIVERSITY of
ROCHESTER



UNIVERSITY OF
OXFORD

- ✓ Magnetized turbulence & fluctuation dynamo
- ✓ Cosmic ray physics

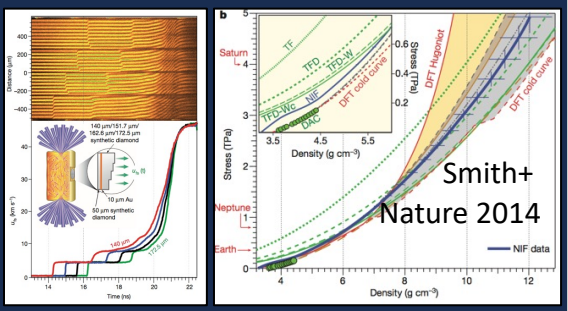
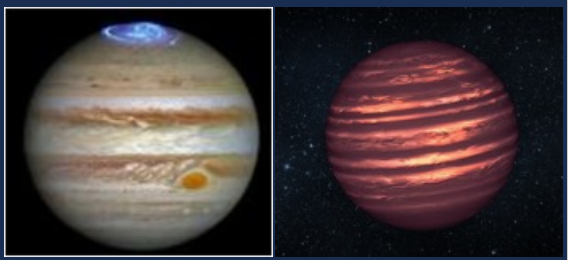
| Astrophysical phenomena & astrophysical systems | $Pm=Rm/Re$ | Cs | Facility | Dates |
|--|------------------|-------|------------------|---------------------|
| Subsonic turbulence: SN shocks, Coma cluster, ISM | < 1 | < 1 | Vulcan (UK) | 2013-2014 |
| Subsonic dynamo: ISM, stars, planets, accretion disks | $< 1, \gtrsim 1$ | < 1 | OMEGA (USA) | 2015-present |
| UHECR transport in turbulent magnetic fields: CR | < 1 | < 1 | OMEGA (USA) | 2016-2020 |
| Subsonic dynamo: IGM, galaxies, galaxy clusters | > 1 | < 1 | NIF (USA) | 2016-present |
| Supersonic turbulence: GMCs, ISM, star formation | < 1 | > 1 | Vulcan (UK) | 2016 |
| Supersonic dynamo: GMCs, ISM, star formation | < 1 | > 1 | OMEGA (USA) | |
| Supersonic turbulence: GMCs, ISM, star formation | < 1 | > 1 | LMJ (France) | |
| Second order Fermi: CR | < 1 | < 1 | GSI (Germany) | |
| NRH instability: CR | < 1 | < 1 | OMEGA+EP (USA) | |



Meinecke et al. submitted (arXiv:2105.08461)

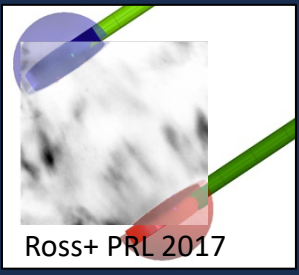
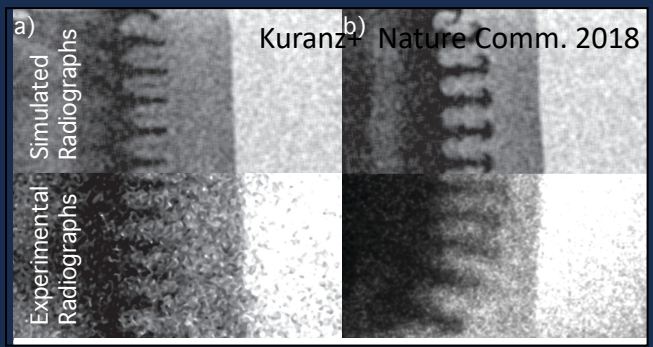
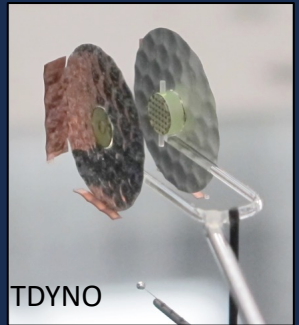
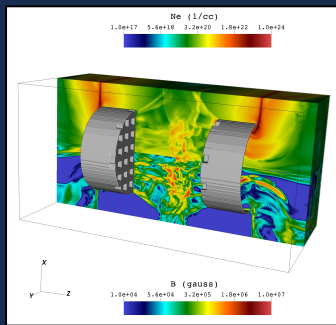
Planetary Science

Planet interiors, equation of state, phase transitions, material properties



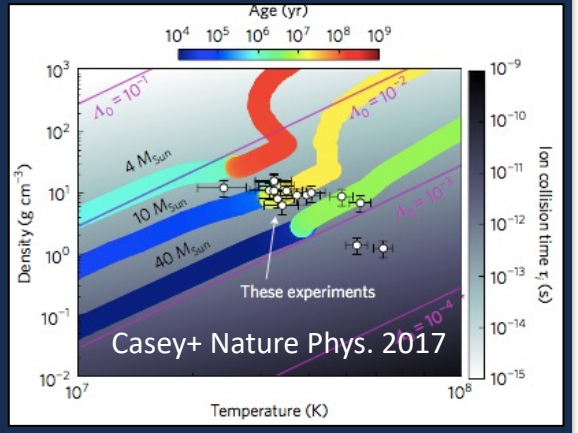
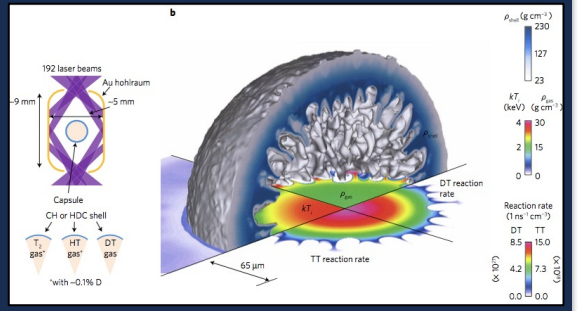
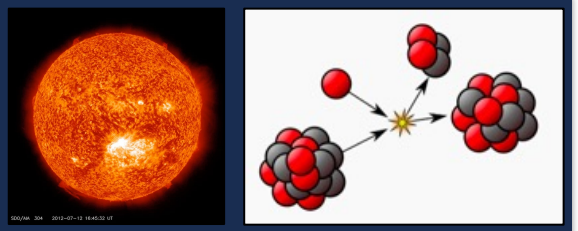
Laboratory Plasma Astrophysics

Shocks, turbulence, particle acceleration and transport, hydro and MHD instabilities

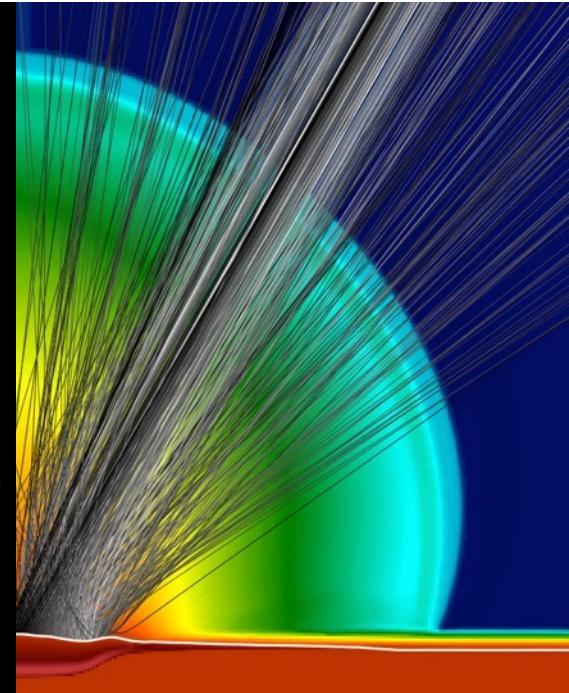
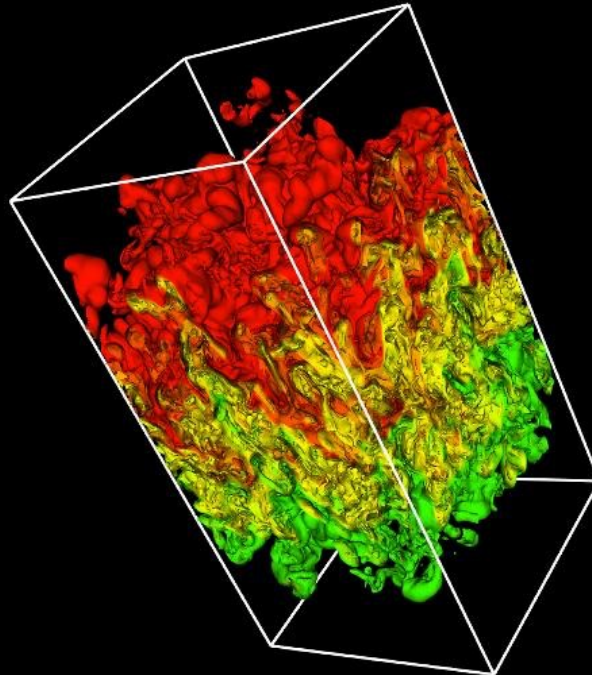
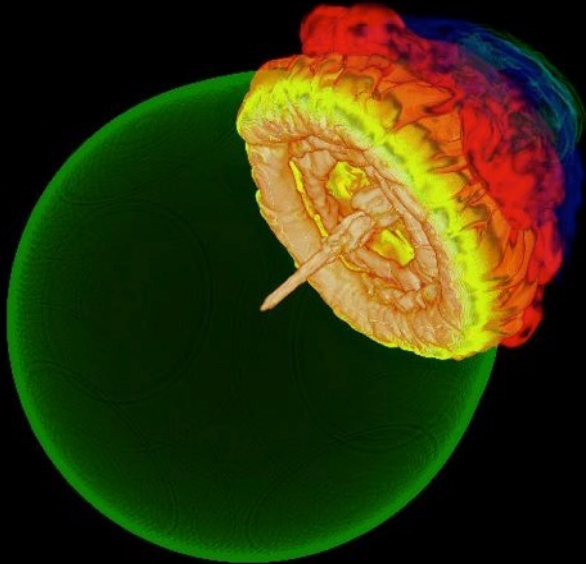


Nuclear Astrophysics

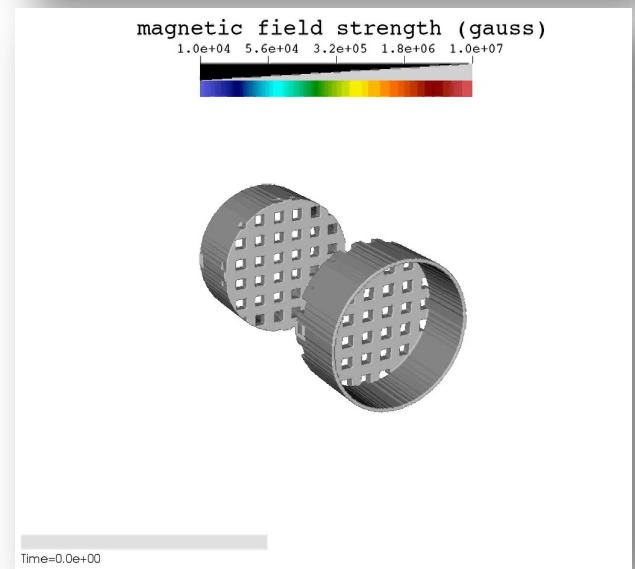
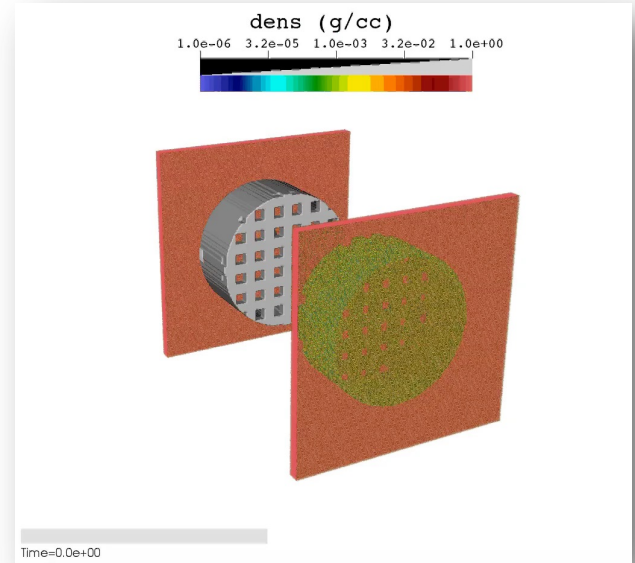
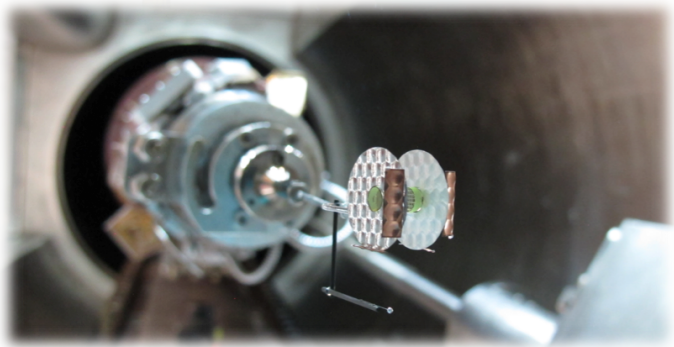
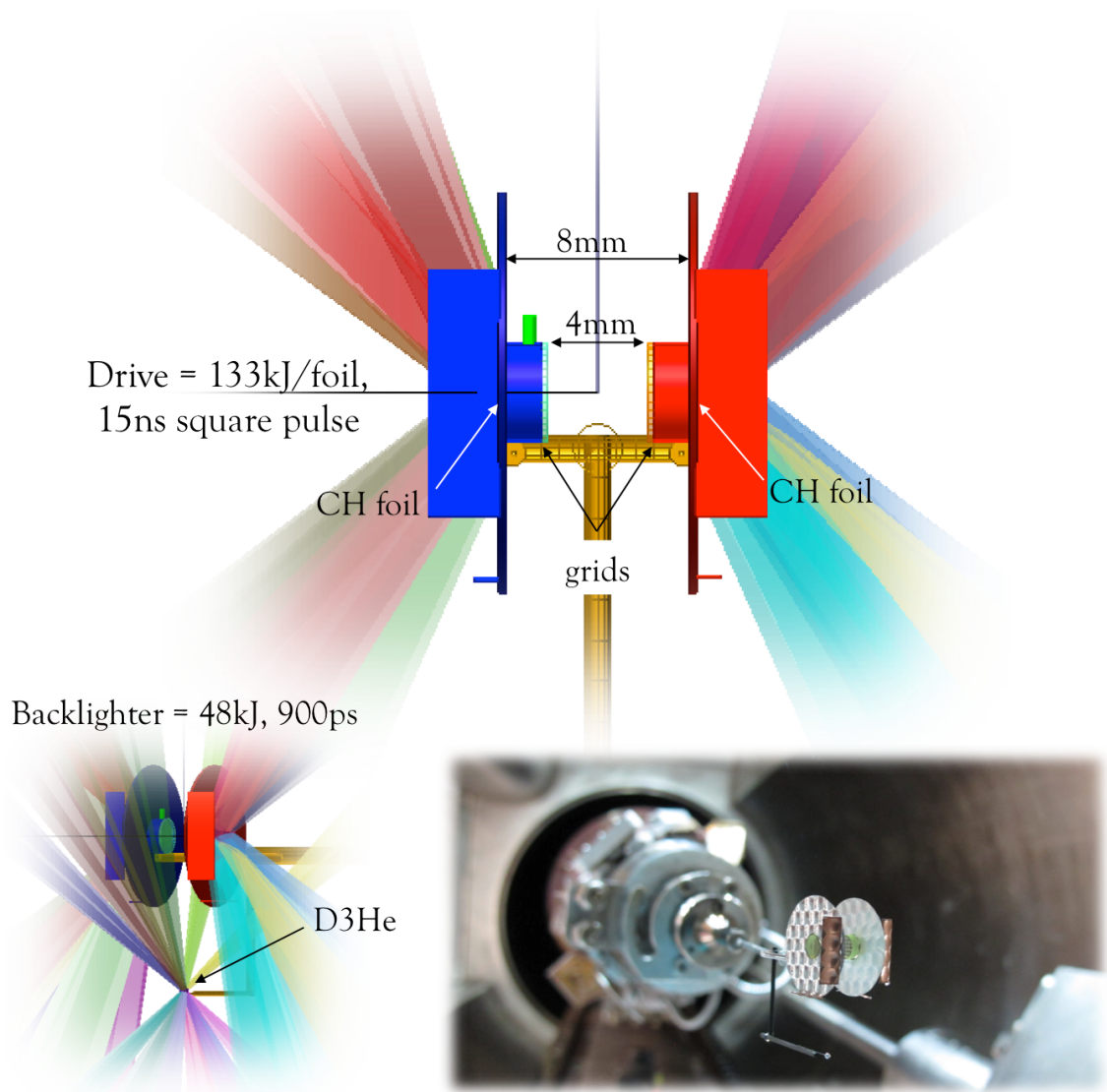
Nuclear reaction rates and cross sections in stellar interiors, s- and r-processes

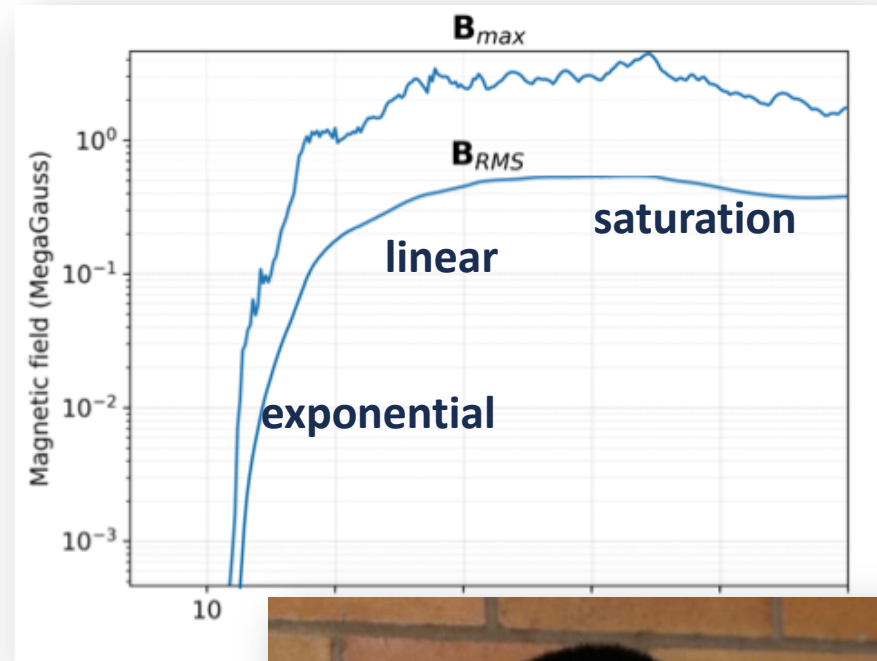
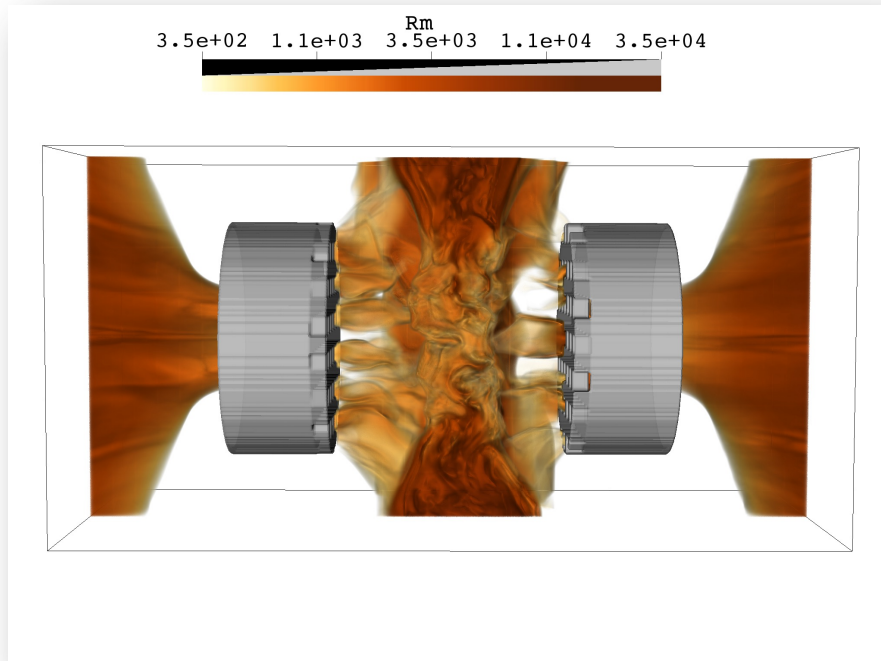


- ❑ FLASH (Fryxell+ 2000) is a publicly available, high-performance computing (HPC), adaptive mesh refinement (AMR), finite-volume, radiation MHD code with extended physics capabilities (Tzeferacos+ 2015). Supported primarily by the **U.S. DOE NNSA, LANL, and LLNL**.
 - ❑ FLASH is professionally managed software in continuous development for 20 years: coding standards; version control; daily automated regression testing; extensive documentation; user support; integration of contributions from external users.
- > 3,500 users worldwide** flash.rochester.edu **>1,200 papers published with FLASH**



Meinecke+ submitted (arXiv:2105.08461)





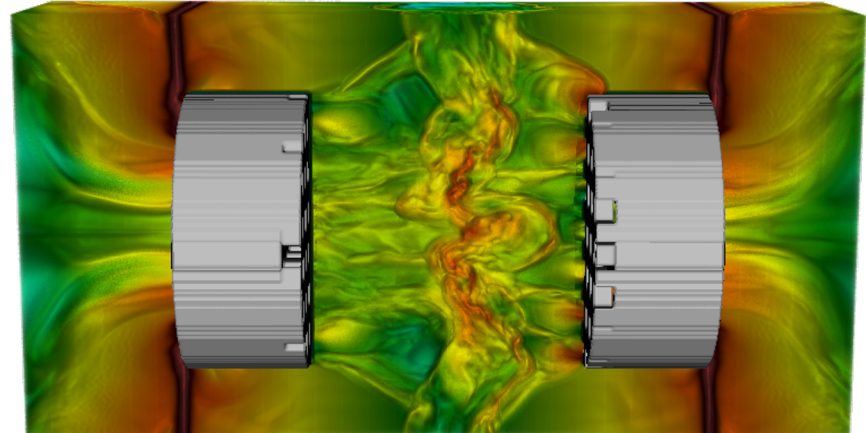
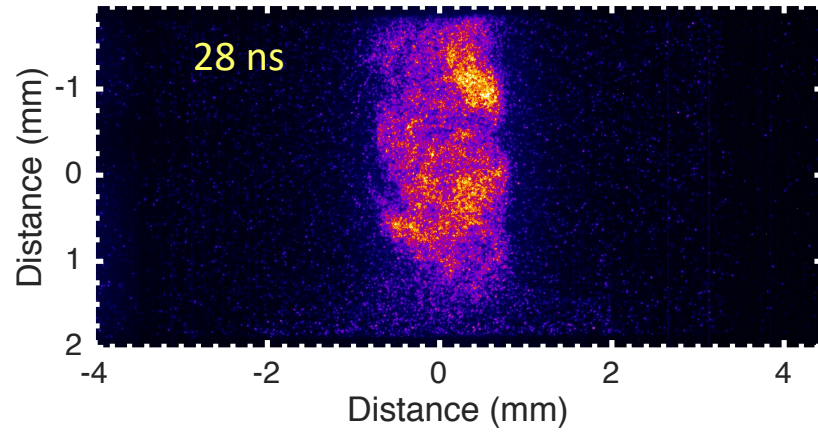
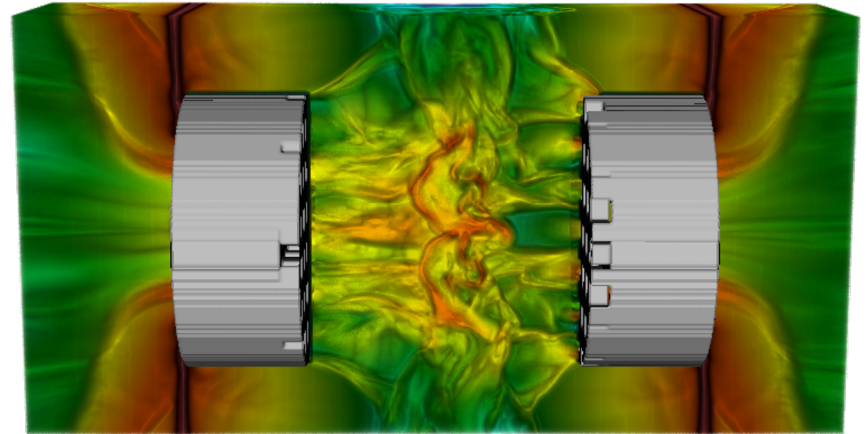
□ The FLASH simulations (Feister+ to be submitted) state with $Pm \gg 1$ and an outer scale $L \sim 600 \mu$ characterized by Rm in the **thousands**, orders of (Schekochihin+ 2004)

□ Within a few ns ($t_{\text{eddy}} \sim L / u \sim 3 \text{ ns}$) the B-field r amplification saturates when the magnetic energy available kinetic energy (RMS)



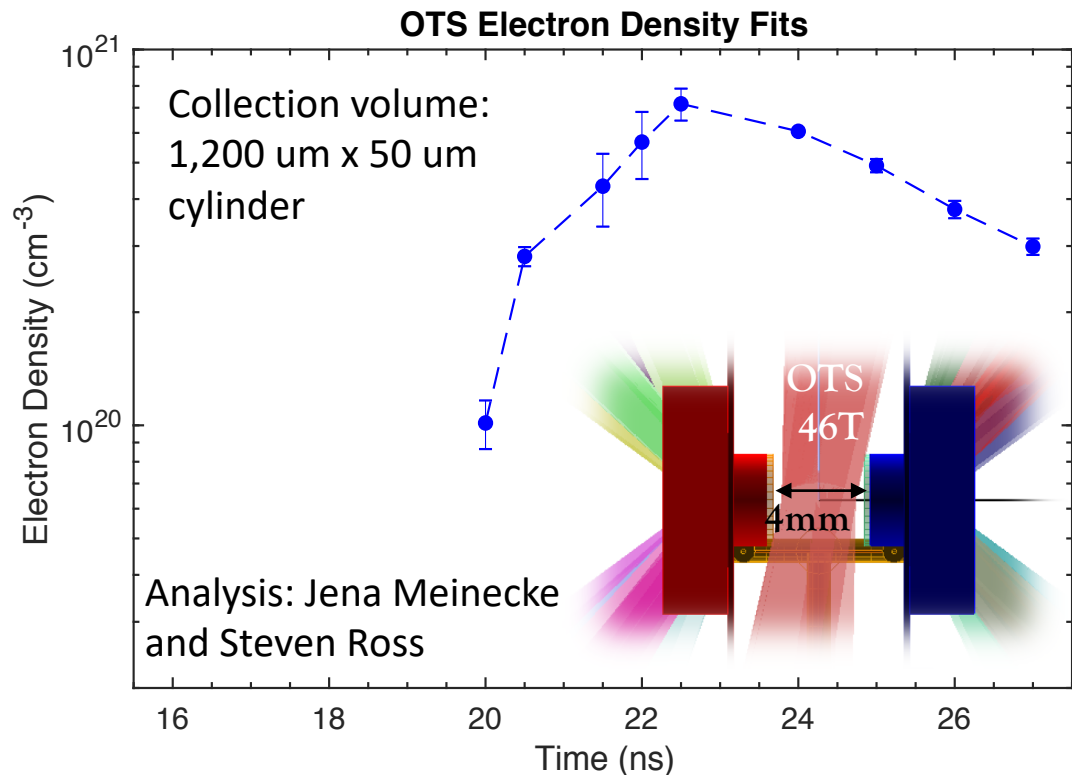
See also the talk by Yingchao Lu!
U003.00011

Distance (mm)

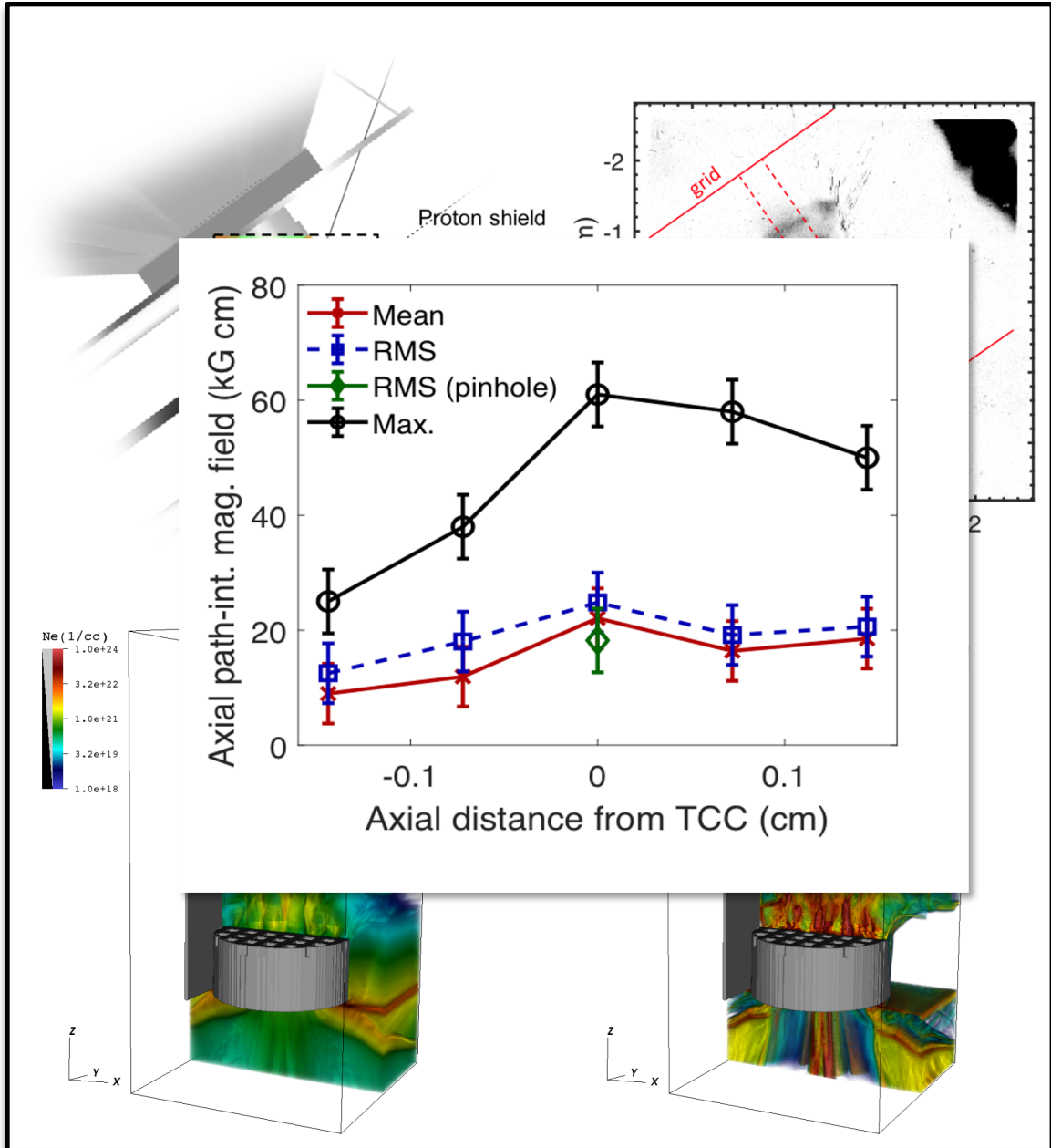


- ❑ X-ray imaging shows the formation of a wide (~ 4 mm), thick ($\sim 1-2$ mm), turbulent interaction region after the interaction of the counter-propagating plasma flows

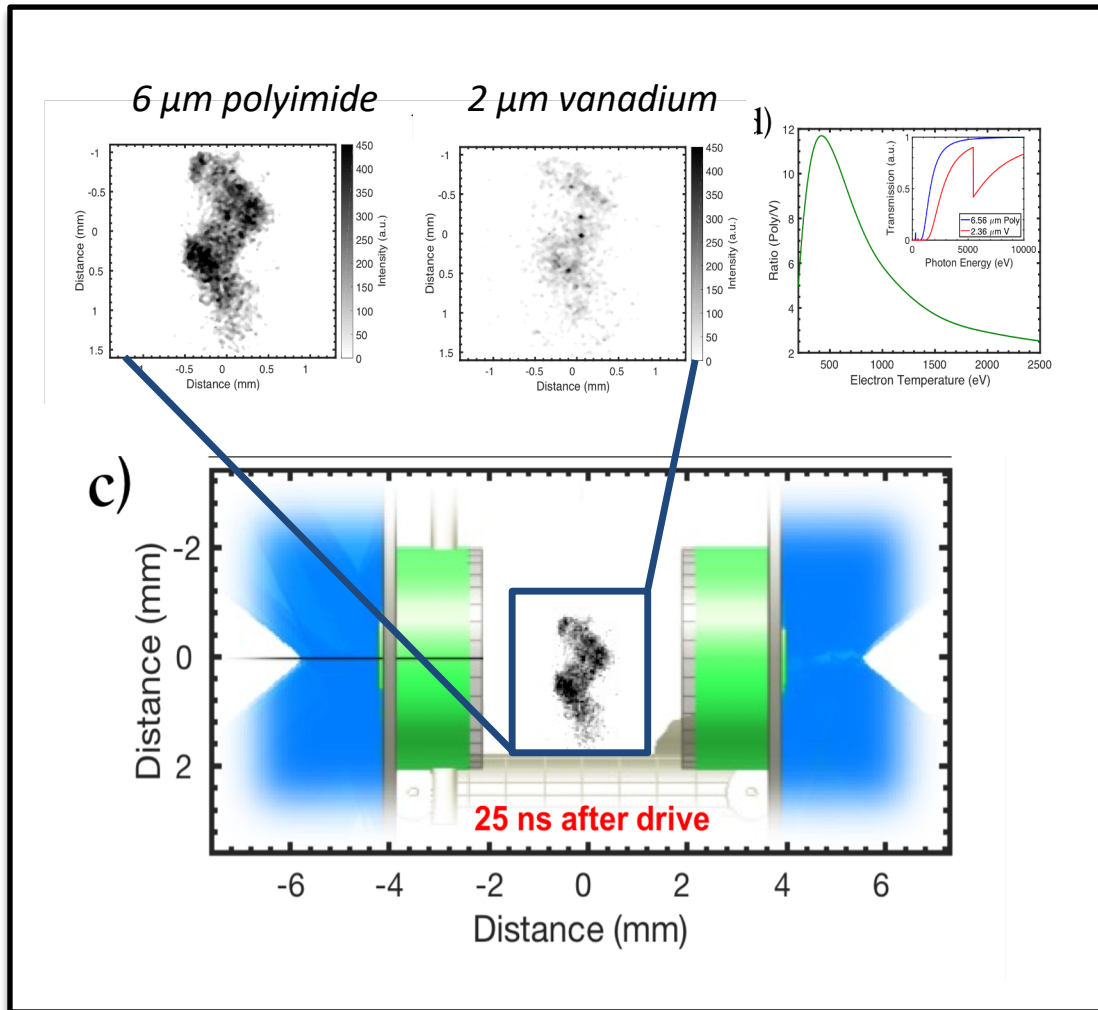
- ❑ The TDYNO campaign fielded NIF's new OTS diagnostic to measure the electron density from the EPW wavelength shifts



- ❑ In the turbulent interaction region, we find $N_e \sim 5 \times 10^{20} \text{ cm}^{-3}$, which is corroborated by FABS; SRS: $N_e \sim 5\text{-}8 \times 10^{20} \text{ cm}^{-3}$, SBS: $u \sim 200 \text{ km/s}$

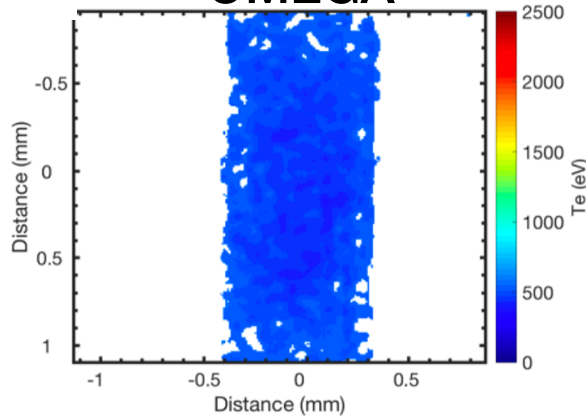


- ❑ PRAD shows protons being **strongly deflected** by the magnetic fields in the plasma.
- ❑ Analysis suggests $B_{\text{rms}} \sim 0.8 \text{ MG}$ and $B_{\text{max}} \sim 2\text{-}3 \text{ MG}$.
- ❑ The magnetic field is strong enough **to suppress thermal conduction**: data shows hot-spots surrounded by cooler plasma.
- ❑ The magnetic field is generated via dynamo action in a turbulent plasma with magnetic Prandtl numbers $Pm \sim 12$ and $Rm \sim 3.5 \times 10^3$.

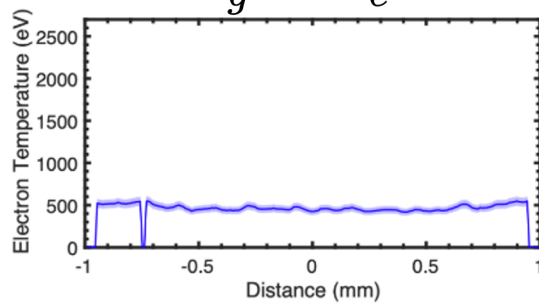


- ❑ Plasma temperature is determined by comparing the X-ray emission in two different energy channels together with the detector response.
- ❑ The technique allows us to create 2D temperature maps of the density weighed path integrated temperature.
- ❑ We validated this technique with synthetic post-processing using SPECT3d and FLASH simulations.

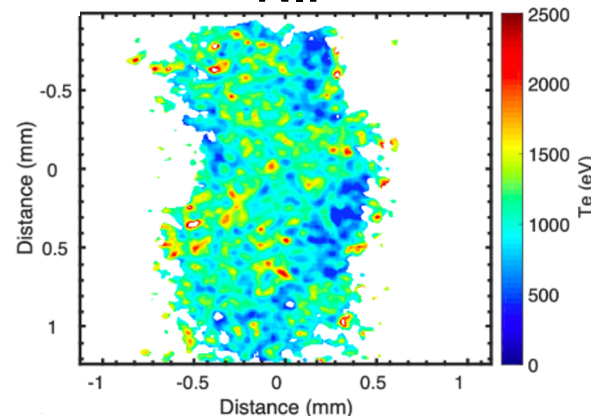
OMEGA



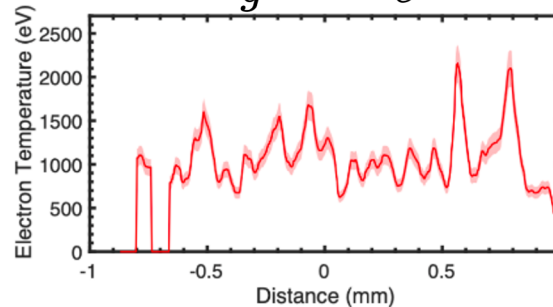
$$r_g > \lambda_e$$



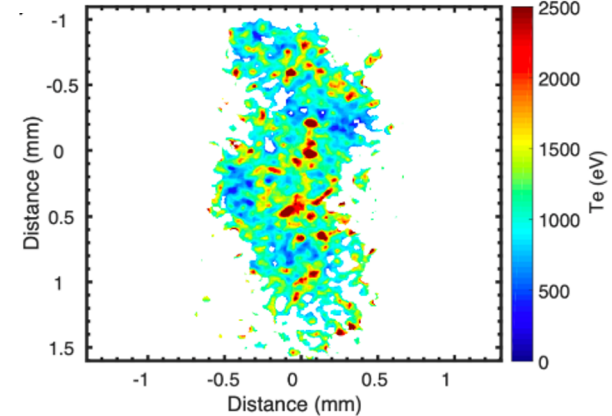
NIF



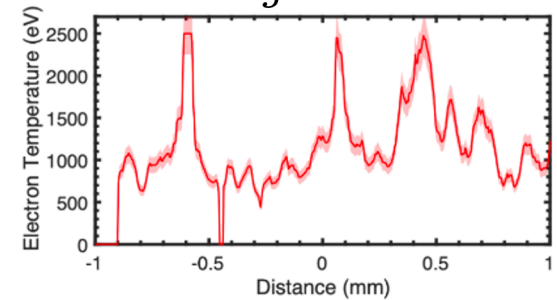
$$r_g < \lambda_e$$



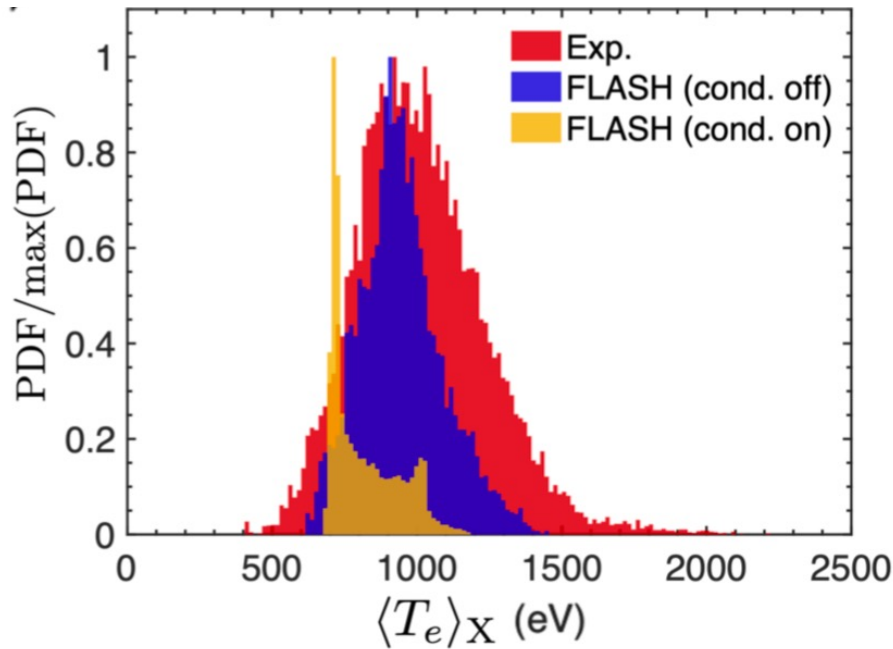
NIF



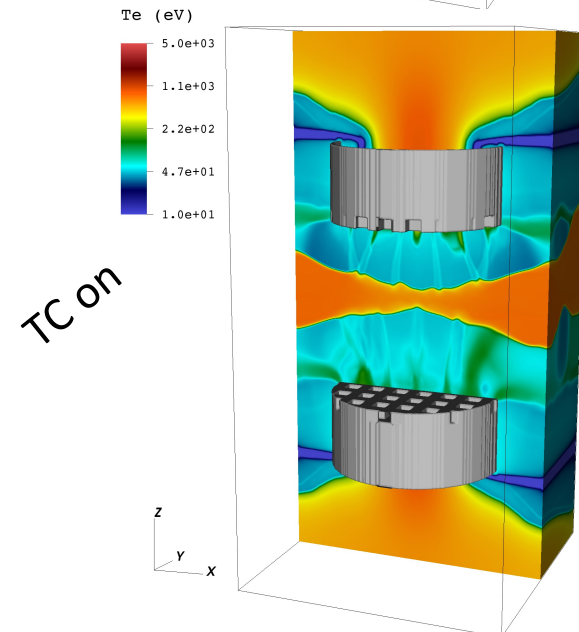
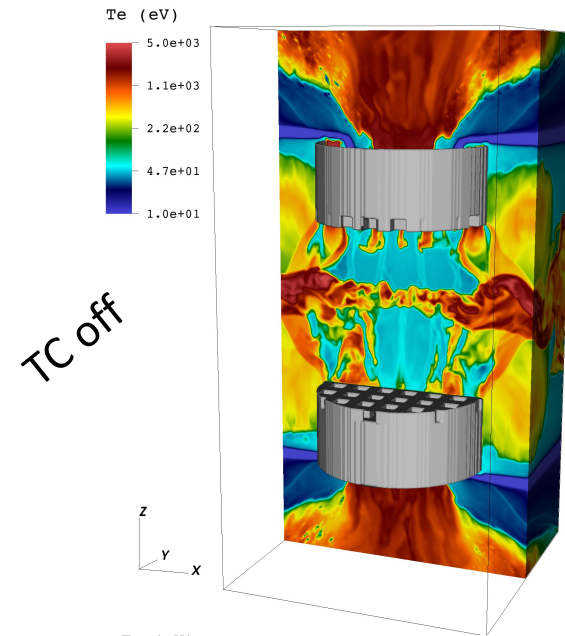
$$r_g < \lambda_e$$



- ❑ NIF data revealed **highly-structured temperature profile** when the Larmor radius, r_g , is smaller than the electron Coulomb mean free path, λ_e
- ❑ The size of hot spots is limited by instrument resolution

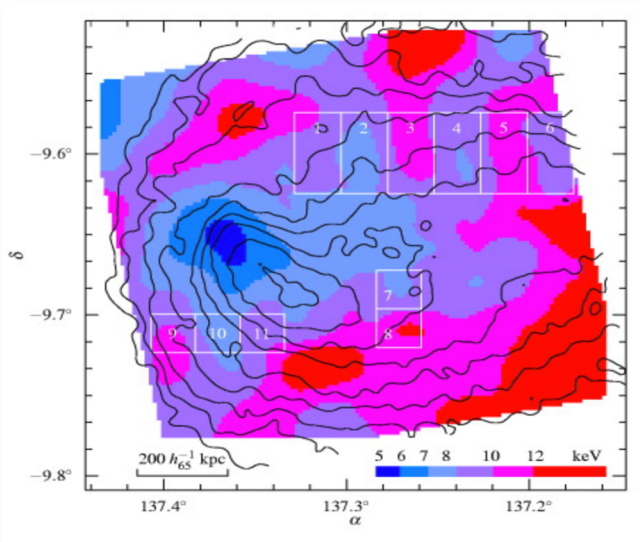


- FLASH simulations show that such a structured temperature profile can be obtained if thermal conduction is uniformly suppressed.
- What is causing this is **not understood** (maybe micro-instabilities, e.g., Komarov+ 2018 and Roberg-Clark+ 2018, for whistler-unstable plasmas).



| Quantity | NIF t = 23ns | NIF t = 25ns | Omega t = 18ns |
|--|-----------------|-----------------|-------------------|
| n_e (cm ⁻³) | 7e20 | 5e20 | 1e20 |
| T_e (keV) | 1.4 | 1.6 | 0.4 |
| l_T (μm) | 50 | 50 | 200 |
| L (mm) | 1 | 1 | 0.5 |
| Z_{eff} | 5.7 | 5.7 | 5.3 |
| t_{cond} (ps) | 27 | 14 | 1324 |
| t_{age} (ns) | 1.7 | 1.6 | 1.6 |
| $\frac{t_{\text{age}}}{t_{\text{cond}}}$ | 63 | 114 | 1.2 |

- An estimate for heat conduction suppression is obtained by comparing the conduction time-scale $t_{\text{cond}} \sim k_B n_e l_T^2 / \kappa_S$ with the time required for the turbulent structures to persist $t_{\text{age}} \sim L / c_s$.
- Our estimates suggest $(\kappa / \kappa_S)^{-1} \sim (t_{\text{age}} / t_{\text{cond}}) > 100\text{-}200\text{x}$ reduction of heat conduction in the NIF experiments.
- These conditions are, in fact, very similar to what we would expect to see in cluster of galaxies and they would potentially be relevant to the problem of cooling flows.

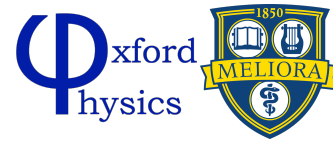


Projected temperature map of A754 overlaid with CHANDRA X-ray image at 0.8-5 keV (Markevitch+ 2003)

- ❑ The advent of high-power lasers has opened **new fields of plasma physics research** and has enabled the reproduction of **astrophysical environments in the laboratory**.
- ❑ The TDYNO platform, which was designed with FLASH simulations to **demonstrate fluctuation dynamo in the lab for the first time**, at the Omega Laser Facility at the Laboratory for Laser Energetics (Tzeferacos+ 2018), has been successfully ported onto the **National Ignition Facility** (Meinecke et al. submitted, arXiv:2105.08461).
- ❑ The NIF experiments achieve fluctuation dynamo in the **large magnetic Prandtl number regime**, an experimental replica for the magnetized turbulence in the IGM.
- ❑ The **strong magnetic fields** generated in the experiments resulted in a **reduction of local heat transport by two orders of magnitude or more**, leading to strong temperature variations on small spatial scales, as is seen in cluster plasmas (Markevitch+ 2003).



TDYNO Collaboration



P Tzeferacos, A Reyes, Y Lu, A Armstrong, K Moczulski



G Gregori, J Meinecke, H Poole, L Chen, T Campbell, A Bell, S Sarkar, F Miniati, A Schekochihin



D Lamb



D Froula, J Katz, D Haberberger, D Turnbull, S Fess (and all LLE staff really!)



H-S Park, JS Ross, T Doepfner, J Emig, C Goyon, D Ryutov, B Remington, A Zylstra



C-K Li, A Birkel, R Petrasso, H Sio, F Seguin

A Bott (Princeton), C Palmer (QUB), B Khair (ONERA), S Feister (CSUCI), A Casner (CEA), D Ryu (Unist), B Reville (MP), C Forest (U Wisconsin), J Foster (AWE), Y Sakawa (Osaka), F Fiuza (SLAC), E Churazov (MPIA), R Bingham (RAL), T White (U Nevada Reno), E Zweibel (U Wisconsin)

Thanks to our sponsors



Engineering and Physical Sciences Research Council

- DOE NNSA, DOE Office of Science, NSF, EPSRC
- DOE's INCITE & ALCC (@ANL), NLUF (@LLE) & DS (@LLNL)
- DOE NNSA NLUF: **DE-NA0002724, DE-NA0003605, DE-NA0003934**
- NSF/DOE Partnership in Basic Plasma & Engineering: **PHY-2033925**
- and General Atomics for target R&D and manufacturing!



Lawrence Livermore National Laboratory

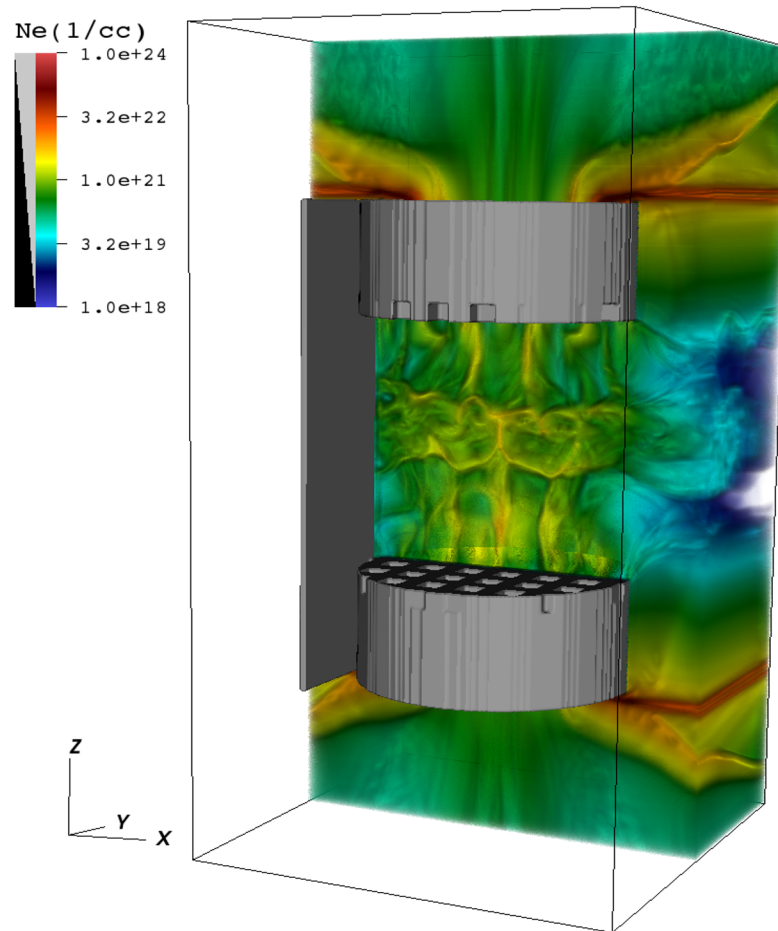
| Quantity | Experimental Value |
|--|---|
| Composition of target | 48.3% C, 49.6% H, 1.2% O, 0.6% N, 0.1% Mn, 0.1% Co |
| Average atomic weight ($\langle M \rangle$) | 6.7 |
| Mean ion charge ($\langle Z \rangle$) | 3.6 |
| Effective ion charge (Z_{eff}) | 5.7 |
| Hydrogen effective ion charge ($Z_{\text{eff,B}}$) | 5.5 |
| Electron temperature (T_e) | 1100 eV |
| Ion temperature (T_i) | 1100 eV |
| Electron number density (n_e) | $4.9 \times 10^{20} \text{ cm}^{-3}$ |
| Turbulent velocity (v_{turb}) | $2 \times 10^7 \text{ cm s}^{-1}$ |
| Outer scale (L) | 0.06 cm |
| RMS magnetic field (B_{RMS}) | 0.8 MG |
| Maximum magnetic field (B_{max}) | 3.0 MG |
| Adiabatic index (γ_I) | 5/3 |

Table 1: Summary of target characteristics and direct experimental measurements of plasma parameters at $t = 25$ ns after the start of the drive laser pulse. The outer scale, L , represents the distance between two neighboring grid aperture centers. Values are reported in CGS, except for the temperature that is given in eV.

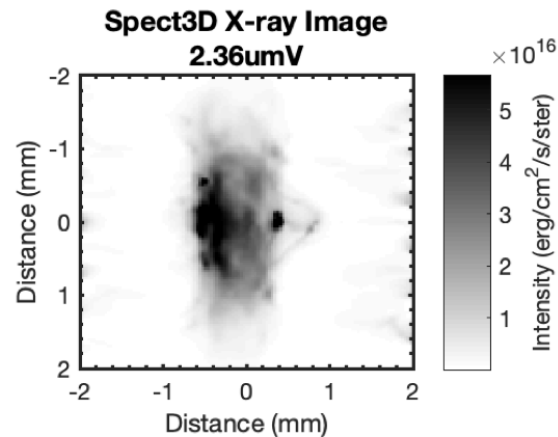
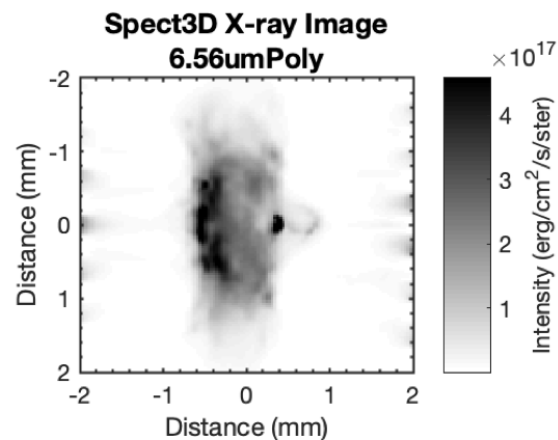
| Quantity | Formula | Value |
|---|---|---|
| Coulomb logarithm ($\log\Lambda$) | $23.5 - \log n_e^{1/2} T_e^{-5/4} - \sqrt{10^{-5} + \frac{(\log T_e - 2)^2}{16}}$ | 7.2 |
| Mass density (ρ) | $1.7 \times 10^{-24} (\sum_j M_j n_j)$ | $1.6 \times 10^{-3} \text{ g cm}^{-3}$ |
| Debye length (λ_D) | $7.4 \times 10^2 \frac{T_e^{1/2}}{n_e^{1/2}} [1 + \frac{T_e}{T_i} Z_{\text{eff}}]^{-1/2}$ | $4.2 \times 10^{-7} \text{ cm}$ |
| Sound speed (c_s) | $9.8 \times 10^5 \frac{[(Z+1)\gamma T_e]^{1/2}}{\langle M \rangle^{1/2}}$ | $3.5 \times 10^7 \text{ cm s}^{-1}$ |
| Mach number | v_{turb}/c_s | 0.6 |
| Plasma β | $4.0 \times 10^{-11} \frac{n_e T_e + \sum_j n_j T_j}{B_{\text{RMS}}^2}$ | 44 |
| H-ion mean free path (λ_{Hion}) | $2.1 \times 10^{13} \frac{T_i^2}{(Z_{\text{H}}^2 Z_{\text{eff,B}} n_e \log \Lambda)}$ | $1.3 \times 10^{-3} \text{ cm}$ |
| Electron-ion mean free path (λ_e) | $2.1 \times 10^{13} \frac{T_e^2}{(Z_{\text{eff}} n_e \log \Lambda)}$ | $1.2 \times 10^{-3} \text{ cm}$ |
| Electron Larmor radius (r_g) | $2.4 \frac{T_e^{1/2}}{B_{\text{RMS}}}$ | $1.0 \times 10^{-4} \text{ cm}$ |
| Hydrogen Larmor radius (ρ_{H}) | $1.0 \times 10^2 \frac{M_{\text{H}}^{1/2} T_i^{1/2}}{Z_{\text{H}} B_{\text{RMS}}}$ | $4.1 \times 10^{-3} \text{ cm}$ |
| Unmagnetized thermal diffusivity (χ_{S}) | $3.0 \times 10^{21} \frac{T_e^{5/2}}{Z_{\text{eff}} n_e \log \Lambda}$ | $5.9 \times 10^6 \text{ cm}^2 \text{ s}^{-1}$ |
| Magnetized thermal diffusivity (χ_{m}) | $\chi_{\text{S}} r_g / \lambda_e$ | $4.7 \times 10^5 \text{ cm}^2 \text{ s}^{-1}$ |
| Suppressed thermal diffusivity (χ) | $\sim \chi_{\text{S}} / 150$ | $3.9 \times 10^4 \text{ cm}^2 \text{ s}^{-1}$ |
| Turbulent Péclet number (Pe_{turb}) | $v_{\text{turb}} L / \chi$ | ~ 30 |
| Dynamic viscosity (μ) | $4.27 \times 10^{-5} \frac{M_{\text{H}}^{1/2} T_i^{5/2} n_{\text{H}}}{\log \Lambda Z_{\text{eff,B}} n_e}$ | $7 \text{ g cm}^{-1} \text{ s}^{-1}$ |
| Kinematic viscosity (ν) | μ / ρ | $4.3 \times 10^3 \text{ cm}^2 \text{ s}^{-1}$ |
| Turbulent Reynolds number (Re_{turb}) | $v_{\text{turb}} L / \nu$ | 280 |
| Viscous dissipation scale (l_ν) | $L / \text{Re}_{\text{turb}}^{3/4}$ | $8.8 \times 10^{-4} \text{ cm}$ |
| In-flow Resistivity (η_{\parallel}) | $3.1 \times 10^5 \frac{Z_{\text{eff}} \log \Lambda}{T_e^{3/2}}$ | $350 \text{ cm}^2 \text{ s}^{-1}$ |
| Magnetic Reynolds number (Rm_{turb}) | $v_{\text{turb}} L / \eta_{\parallel}$ | 3.5×10^3 |
| Magnetic Prandtl number (Pm) | Rm / Re | 12 |
| Resistive dissipation scale (l_η) | $L / \text{Pm}^{1/2}$ | $2.5 \times 10^{-4} \text{ cm}$ |

Table 2: Summary of derived plasma parameters at $t = 25 \text{ ns}$ after the start of the drive laser pulse. The values are reported in CGS.

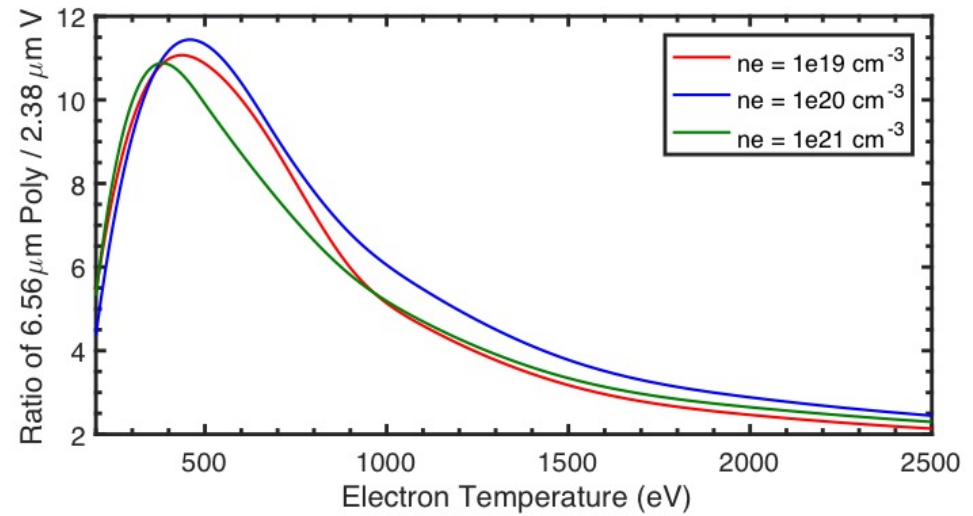
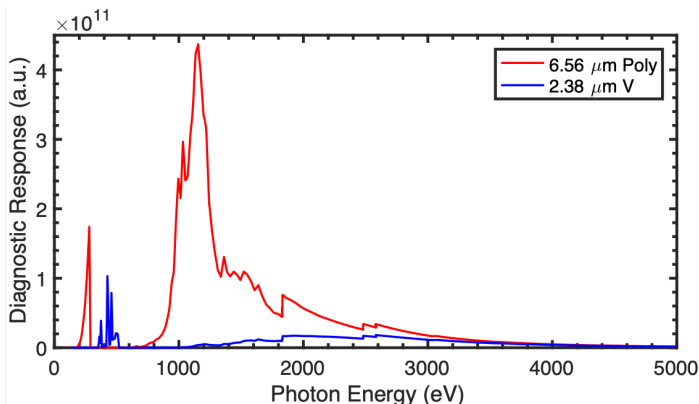
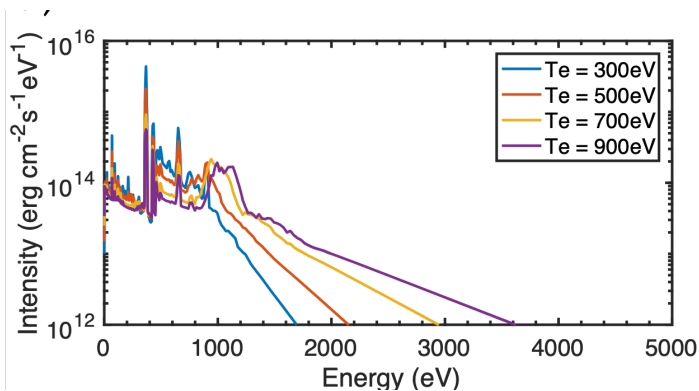
- **Step 1:** We take FLASH simulations results for the interaction region.



- ❑ **Step 1:** We take FLASH simulations results for the interaction region.
- ❑ **Step 2:** FLASH simulations are post-processed using SPECT3d to obtain synthetic X-ray maps of the interaction region.



- ❑ **Step 1:** We take FLASH simulation results for the interaction region.
- ❑ **Step 2:** FLASH simulations are post-processed using SPECT3d to obtain synthetic x-ray maps of the interaction region.
- ❑ **Step 3:** A relation between filter ratio and temperature is obtained by running PrismSPECT for a range of different plasma conditions.



- ❑ **Step 1:** We take FLASH simulations results for the interaction region.
- ❑ **Step 2:** FLASH simulations are post-processed using SPECT3d to obtain synthetic x-ray maps of the interaction region.
- ❑ **Step 3:** A relation between filter ratio and temperature is obtained by running PrismSPECT for a range of different plasma conditions.
- ❑ **Step 4:** The mass-weighted (along the line-of-sight) temperature map obtained from the filter ratio is compared to the mass-weighted temperature from FLASH simulations.

